

Surface Organization of Hyperbranched Polymer Molecules, as Studied by Atomic Force Microscopy

Pascal Viville*¹, Alain Deffieux², Michel Schappacher², Philippe Leclère¹, Jean-Luc Brédas^{1,3} and Roberto Lazzaroni¹

¹Service de Chimie des Matériaux Nouveaux, Centre de Recherche en Sciences des Matériaux Polymères (CRESMAP), Université de Mons-Hainaut 20, Place du Parc, 7000 Mons, Belgium

²Laboratoire de Chimie des Polymères Organiques, UMR ENSCPB-CNRS 5629 Université de Bordeaux 1, Avenue Pey Berland BP108, 33405, Talence, France

³ Department of Chemistry, The University of Arizona, Tucson, Arizona 85721-0041, USA

SUMMARY:

The recent emergence of hyperbranched polymers has opened the door for the design of a large variety of novel, well-controlled chain architectures. For instance, «comb-like» and "dendritic-like" polymers can be obtained from hyperbranched poly(chloroethyl vinyl ether)-g-polystyrene (PCEVE-g-PS) copolymers, with excellent control over the dimensions of the polystyrene lateral branches and the PCEVE backbone. In this work, the nanometer scale organization of these materials is studied by means of Tapping Mode Atomic Force Microscopy. We focus on the influence of the intrinsic molecular architecture of the hyperbranched PCEVE-g-PS on the organization of the material. In the case of thin deposits, we observe a layer-by-layer organization. On the free surface, it is possible to image single polymer molecules and to analyze their size in terms of polymer molecular weight. In most cases, the molecules are found to adopt an extended conformation and to form lamellar arrangements. We observe that the degree of lateral ordering of these molecules strongly depends on their intrinsic architecture.

Introduction

Polymer chemistry has long focused on linear macromolecules, which occasionally contain some smaller or longer branches. In recent years, highly-branched polymers have gained widespread attention due to their unique properties, which can differ significantly from their linear counterparts; e.g., the large number of terminal functional groups, the intrinsic

* Corresponding author: tel : +32 65 373868; fax: +32 65 373861; e-mail: Pascal@averell.umh.ac.be

globular structure (leading to specific rheological properties), and the possibility to accommodate guest molecules within the macromolecule. Compared to dendrimers, hyperbranched macromolecules are characterized by a lower degree of branching, but still possess a non-linear molecular architecture and a high number of potentially reactive end groups. Moreover, they can be prepared much more rapidly and economically than dendrimers and are therefore considered as very good candidates to replace dendrimers in a number of applications ¹⁻³.

An important research activity has been devoted in recent years to the development of new synthetic procedures allowing the preparation of branched and hyperbranched polymers with tailored molecular architecture and well-controlled dimensions as, for instance, star- and comb-like polymers. Recently, a new route to the preparation of comb-like and dendritic-like architectures has been proposed. The method is based on the branching of polystyrene onto poly(chloroethyl vinyl ether) backbone, yielding poly(chloroethyl vinyl ether-g-styrene) (PCEVE-g-PS) copolymers. With this method, both first generation and hyperbranched analogous (second generation) copolymers can be prepared. The dimensions of the grafted PS branches and the PCEVE main backbones can be controlled with great accuracy by living polymerization so that both the length and the number of branches of the graft copolymers can be tuned ⁴⁻⁶. As a consequence, different chain architectures can be generated, that are expected to arrange into different supramolecular assemblies.

In this work, the molecular organization of (PCEVE-g-PS) copolymers in thin solid films is characterized by Tapping Mode Atomic Force Microscopy (TMAFM), which probes the surface topography with very high lateral resolution. Recently, AFM was shown to be a powerful technique to study the morphology of comb-like polymer molecules and to determine their molecular characteristics, such as absolute molar mass, molar mass distribution and chain conformation ⁷⁻⁸. It has been demonstrated that comb-like polymers (or polymer brushes) can change their conformation from statistical coils to wormlike cylindrical brushes as a result of sterical hindrance due to the numerous grafted segments ⁹. The influence of the nature and the size of the side chains on the surface organization of the polymer brush has already been examined theoretically ¹⁰. In this work, we show experimentally how a significant change in side-chain complexity dramatically modifies the way PCEVE-g-PS

molecules organize in the solid state. We also address the important question of the influence of sample preparation conditions on this molecular organization.

Experimental section

PCEVE-*g*-PS copolymers have been synthesized by living polymerization via a grafting reaction of polystyryl lithium segments onto poly(chloroethyl vinyl ether) chains. The selectivity of the coupling reaction is very high and allows for complete substitution of the chloride group of the initial CEVE units by PS chains, thus allowing the synthesis of comb-like polymers. Using the first generation copolymers as multifunctional CEVE polymerization precursors, we could repeat the whole procedure in order to get the corresponding hyperbranched copolymers of second generation. The reaction schemes involving the preparation of the PCEVE backbone and the polystyryl lithium grafting in the case of the first and the second generation copolymers are described in recent publications ⁴⁻⁶.

In this work, two copolymers with different side-chain complexity (generation 1 and generation 2) are considered (Fig. 1).

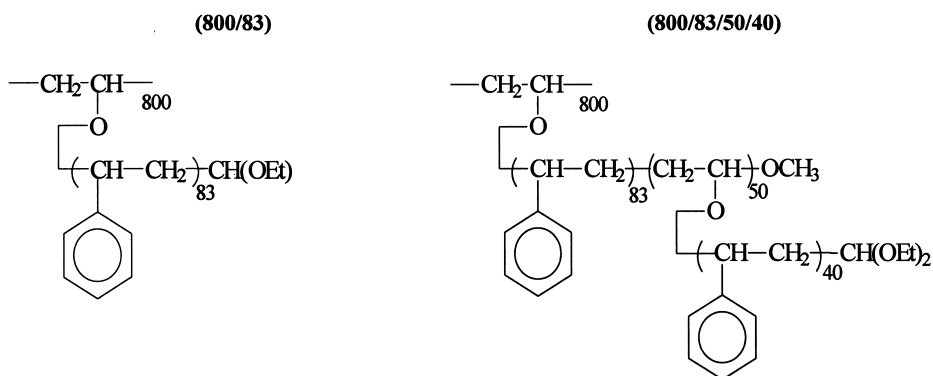


Fig. 1 : Molecular architecture of the (800/83) and (800/83/50/40) PCEVE-*g*-PS grafted copolymers.

Table 1 shows some typical structural and dimensional characteristics of the two copolymers shown here above.

Table 1: Typical dimensional and solution characteristics of the first and second generation PCEVE-g-PS copolymers

Constitutive blocks (\overline{DP}_n)	\overline{Mn}_{th} 10^{-6}	$\overline{Mn}_{app}^{a)}$ SEC (RI) 10^{-6}	$\overline{Mw}_{exp}^{b)}$ SEC (LS) 10^{-6}	$\overline{M}_w / \overline{M}_n$	$[\eta]^c)$ dl/g	Rh (nm)	Rg (nm)
800-83	6.5	0.99	5.4	1.06	0.46	34.6	45.0
800-83-50-40	175.0	2.7	120.0	1.13	0.19	71.0	78.0

a) determined by SEC using PS standards; b) determined by light scattering in THF; c) measured at 25°C in THF

Samples for AFM analysis are prepared by solvent casting at ambient conditions starting from solutions in tetrahydrofuran (THF). Typically, 50 μ l of a dilute solution at various concentrations (from 0.01 wt % up to 0.1 wt%) is cast on a 1 x 1 cm² surface of a freshly-cleaved mica substrate. The samples are analyzed after complete evaporation of the solvent at room temperature.

All AFM images are recorded in air with a Nanoscope IIIa microscope operated in Tapping Mode (TM). The probes are commercially available silicon tips with a spring constant of 24-52 N/m and a resonance frequency lying in the 264-339 kHz range. In this work, both the topography and the phase signal images are recorded with the highest sampling resolution, *i.e.*, 512 x 512 data points.

Results and Discussion

Fig. 2 shows 750 x 750 nm² TM-AFM phase images of (800/83) and (800/83/50/40) PCEVE-g-PS copolymer thin films prepared from 0.1 wt% solutions in THF and deposited on mica. The observed surface morphology is homogeneous over a large scale. The film thickness is around 50 nm for the two compositions. A closer inspection of these multilayered deposits reveals that the two copolymers are characterized by a well-defined morphology on the nanometer scale, made of long objects assembled parallel to each other, along with regions where these objects fold (for instance, the bright feature marked by an arrow in the left image).

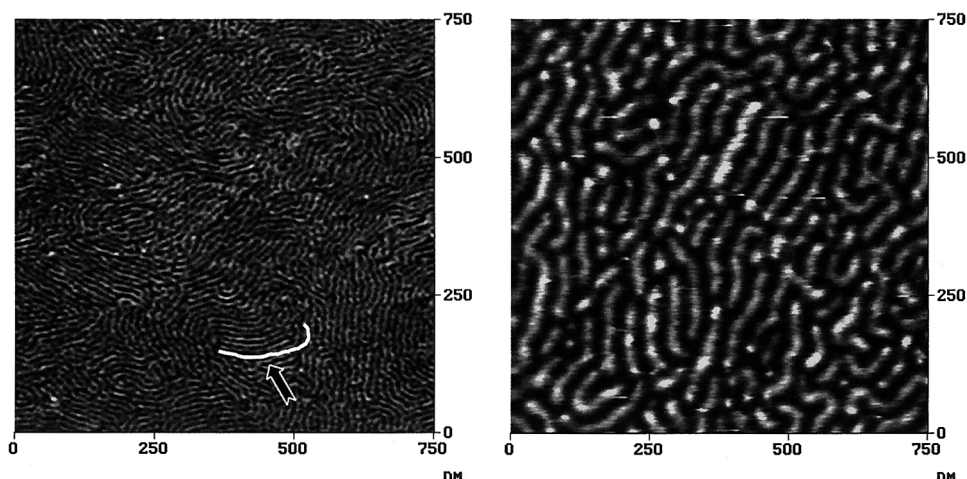


Fig. 2: TM-AFM phase images ($750 \times 750 \text{ nm}^2$) of the surface morphology of the (800/83) copolymer (left) and the (800/83/50/40) copolymer (right).

Such a morphology is attributed to the intrinsic “comb-like” molecular architecture of the copolymers that forces the macromolecules to adopt a conformation of wormlike cylindrical brushes (illustrated in Fig. 3, left). The cylindrical brush conformation is induced by the large sterical hindrance caused by the presence of numerous PS grafted segments that decrease the flexibility of the main PCEVE chain. The intermolecular ordering observed in Fig. 2 is controlled by the sterical repulsion between the grafted PS chains, which means that the distance between two neighboring cylinders in the images corresponds to the distance between two neighboring PCEVE backbones. Note that the cylindrical brush conformation observed here for PCEVE-g-PS copolymer chains is fully consistent with the results of recent works ^{7, 8}.

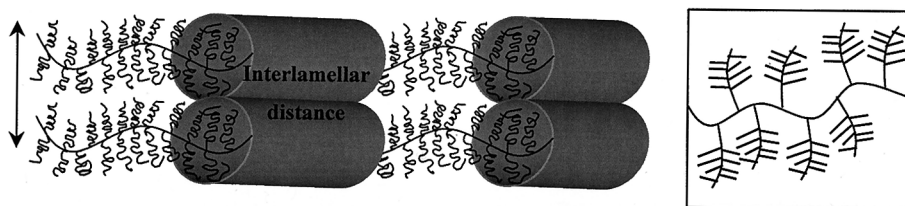


Fig. 3: Schematic view of the cylindrical brush conformation. The inset shows a schematic representation of the more complex molecular architecture of the (800/83/50/40) copolymer.

A fundamental information revealed by the AFM images is the large increase in cylinder thickness observed when the structural complexity of the lateral side chain is modified from that of a first generation (800/83) to a second generation (800/83/50/40) grafted copolymer. In the latter case, each lateral segment consists of a « comb-like » structure, bound to a common backbone (see right inset in Fig. 3). The higher steric hindrance of these longer and bulkier side chains causes the average cylinder thickness to increase from 13 nm for the (800/83) copolymer up to 40 nm for the (800/83/50/40) copolymer. In most cases, the cylinders appear as continuous objects within which interruptions are discernable. Considering that these interruptions are molecules ends and that, as an extreme case, a fully extended PCEVE backbone with 800 monomer units yields a value of ~200 nm for the chain contour length, we conclude that the objects appearing within the features in the two images of Fig. 2 are indeed single molecules.

As a further step in the characterization of the surface organization of these copolymers, we considered samples prepared from more dilute solutions (0.01 wt % in THF) with the aim of observing the intrinsic morphology of the copolymers in flat monolayers. Under these conditions, the solution dewets from the mica substrate during the drying process as a consequence of the weak affinity between the copolymer solution and the hydrophilic substrate. As an example, Fig. 4 shows a series of topographic AFM images illustrating the large scale dewetting process observed in the case of the (800/83) copolymer. These images correspond to snapshots of the situation after the solvent has completely evaporated from the sample and show deposits of the copolymer, appearing here as the bright features, on the mica surface. They illustrate that the dewetting is not homogeneous on the whole surface and can lead either to a strongly interconnected morphology (4a), to isolated islands (4c), or to intermediate situations where both types of morphology coexist (4b). It also appears from the coexistence on the same surface of these three morphologies that the formation of smaller, taller islands (4c) is generated through further dewetting of larger deposits. This heterogeneity in the deposits indicates that the structures that are generated during the dewetting process strongly depend on the local kinetics of the solvent evaporation and that these kinetics are not equivalent over the whole sample. Under these conditions, the morphology shown in image 4a would correspond to a more rapidly frozen structure and that in image 4c to a more accomplished dewetting process.

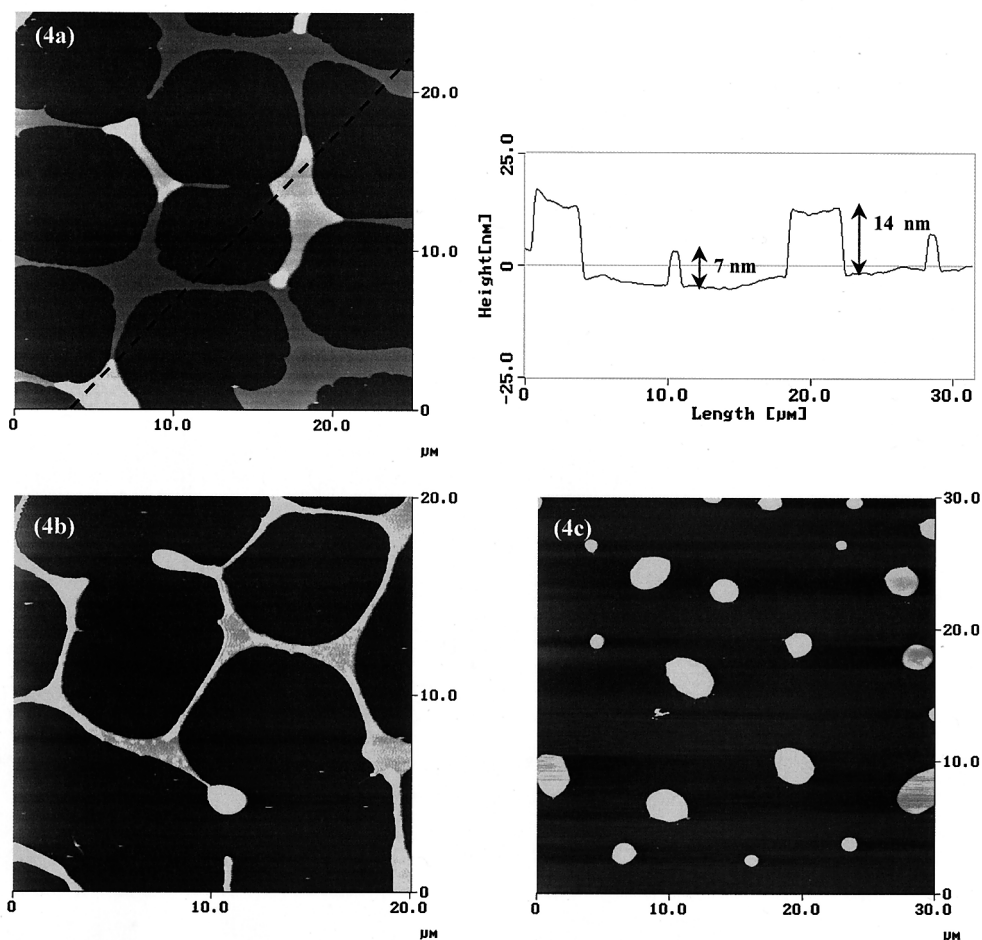


Fig. 4: TM-AFM topographic images ($25 \times 25 \mu\text{m}^2$, $20 \times 20 \mu\text{m}^2$ and $30 \times 30 \mu\text{m}^2$) of the multilayer organization for the (800/83) copolymer prepared from a 0.01 wt% solution. The vertical scale is 25 nm for the three images.

A direct consequence of this fact is that the dewetting process leads to the formation of layered deposits. A cross-section analysis of the structures (for instance; along the black dashed line in image 4a) reveals areas that exhibit the same height. The analysis also reveals that the brighter areas have twice the height of the gray zones: the gray areas in image 4a correspond to a flat, 7 nm-thick, layer of the (800/83) copolymer while the brightest zones are 14 nm-thick deposits. As the dewetting proceeds a step further, thicker deposits are formed, such as the 20 nm-thick isolated deposits shown in image 4c. This multiplicity in the height of the layers and the fact that no feature thinner than 7 nm has been observed suggest that the 7 nm-thick layer represents a monolayer of the (800/83) copolymer. The thicker deposits thus

correspond to bilayers and trilayers. The different multilayered topographies shown in Fig. 4 can thus be interpreted as the consequence of a kinetically-controlled dewetting process of copolymer monolayers.

This multilayered deposit organization is observed for the two types of copolymer. Fig. 5 and Fig. 6 show high magnification images of the monolayers for the (800/83) and the (800/83/50/40) copolymers, respectively. Cross-section analysis across these images shows that monolayers of the (800/83/50/40) copolymer are much thicker than for the (800/83) copolymer, i.e; 26 nm vs 7 nm, which is consistent with the increase in sterical hindrance of the side chains in the case of the second generation (800/83/50/40) copolymer. This result shows that a change in copolymer molecular architecture strongly affects the thickness of the corresponding monolayers.

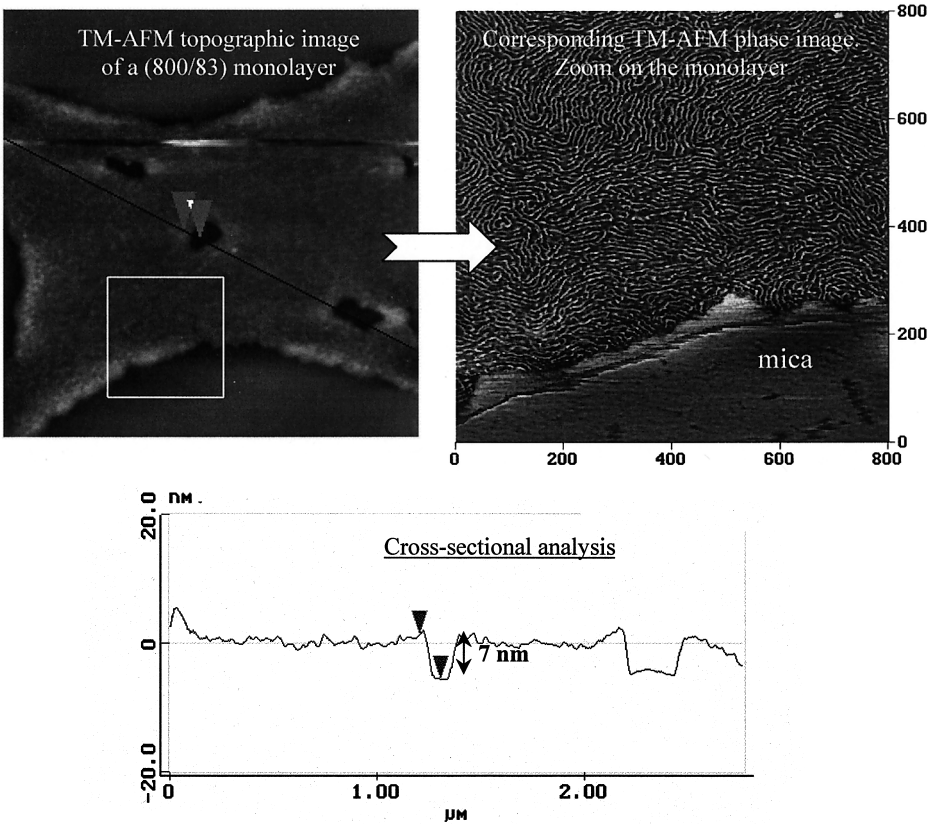


Fig. 5: Top: TM-AFM topographic image ($2.5 \times 2.5 \mu\text{m}^2$) of one monolayer of the (800/83) copolymer (left) and phase image ($800 \times 800 \text{ nm}^2$) on the monolayer (right). Below: Cross-sectional analysis of the monolayer.

Within these monolayers, the chains are also found to be organized into a densely packed cylindrical brush conformation. The same differences in the molecular width between the two compositions are also found, which is coherent with our previous observations. It must be noted that, for deposits on mica, the measured height and width of the molecules are significantly different, which suggests that the brushes are ellipsoidal rather than cylindrical.

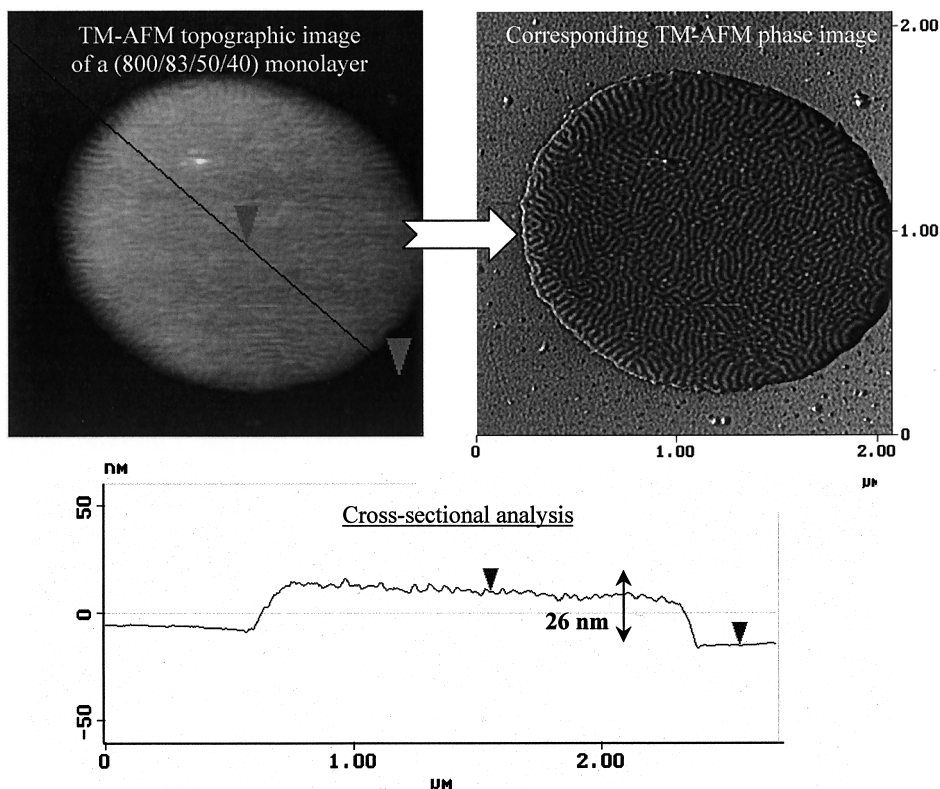


Fig. 6: Top: TM-AFM topographic image ($2.1 \times 2.1 \mu\text{m}^2$) of a monolayer of the (800/83/50/40) copolymer (left) and corresponding phase image ($2.1 \times 2.1 \mu\text{m}^2$) (right). Below: Cross-sectional analysis of the monolayer.

As a further step, we investigated the areas located between the heterogeneous deposits generated by the dewetting. The AFM measurements reveal the presence of very small isolated structures that seem to have been “left behind” on the mica during the dewetting process. These isolated features are repeatedly found on the surface of different samples prepared in the same conditions. As an example, Fig. 7 shows an area with a deposited island

of the (800/83) copolymer and the uncovered mica surface, revealing the presence of small particles around the deposit.

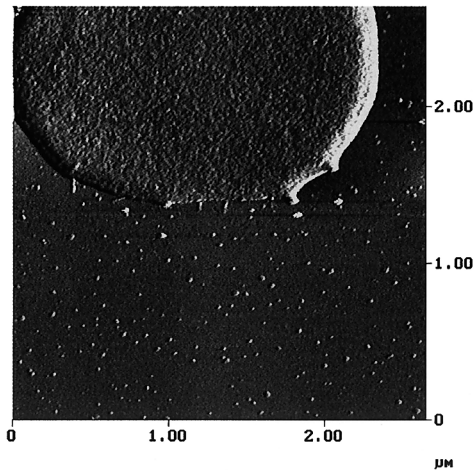


Fig. 7 : TM-AFM phase image showing a deposited island of the (800/83) copolymer and the uncovered mica surface.

When zooming in on such an area (Fig. 8), it clearly appears that all these small objects are similar in size and shape: they are round-shaped and exhibit a different response in their middle. In our opinion, these objects are single (PCEVE-g-PS) copolymer molecules considering their uniformity of size and shape.

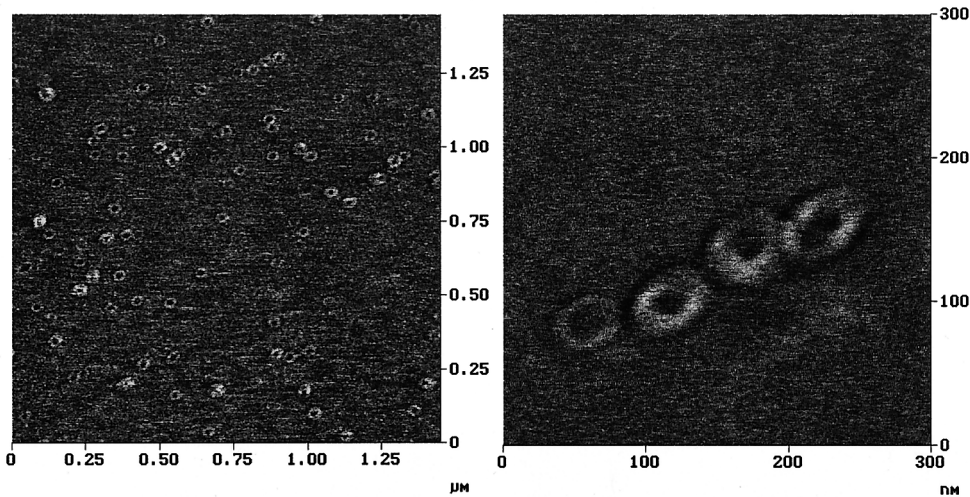


Fig. 8: TM-AFM phase images ($1.5 \times 1.5 \mu\text{m}^2$ and $300 \times 300 \text{ nm}^2$) of isolated molecules of the (800/83) copolymer.

Along the same line, isolated small features of the second generation (800/83/50/40) copolymer were also found lying on the free mica surface after deposition from a 0.01 wt % solution. Compared to the (800/83) copolymer, the features are also round-shaped but they are however larger in size and do not exhibit a « doughnut-like » morphology.

The diameter distribution of these objects is statistically determined for a set of different AFM images. Fig. 9 shows the Gaussian distributions obtained by measuring the diameter of a large number of these objects for the two copolymers. The measurements are carried out on separate samples prepared in the same conditions and using the same TMAFM tip. The diameter distribution of (800/83) copolymer molecules is shown in Fig. 9 as the solid line and the black dots. It yields a most probable diameter at the maximum of the distribution equal to 35.6 nm. This diameter value is in good agreement with the hydrodynamic radius (R_h) of the corresponding copolymer molecules, i.e; 34.6 nm, experimentally determined in THF by Dynamic Light Scattering. Such agreement further indicates that the features seen in Fig. 8 are isolated molecules of the (800/83) copolymer. The molecule size distribution curve corresponding to the (800/83/50/40) copolymer is shown in Fig. 9 as the dashed line and the white dots. The diameter determined at the maximum of the Gaussian distribution is clearly shifted to higher values, from 35.6 nm up to 46.1 nm. Isolated molecules of (800/83/50/40) copolymer molecules are thus much larger in size. This evolution clearly highlights the effect of an increase in molecular architecture complexity and in molecular mass, on the size of individual copolymer molecules observed by AFM.

The “doughnut-like” morphology of isolated (800/83) copolymer molecules is believed to be the result of (i) the weak affinity of the PCEVE-*g*-PS copolymer molecules for a hydrophilic surface such as mica and (ii) the absence of neighboring polymer molecules. This would force the isolated molecules to coil to a certain extent. However, due to the rigidity of the backbone, the chain cannot fully collapse and a void remains in the center. Assuming such a conformation, the contour length of the PCEVE backbone giving rise to the measured diameter is around 130 nm, which is in reasonable agreement with the expected length of the elongated backbone of (800/83) copolymer molecules. Furthermore, the average thickness of the torus of these doughnut-like objects is equal to the thickness of the extended cylindrical brush molecules observed on flat monolayers, 13 nm, which gives a further argument for a coiled conformation of the cylindrical brushes when they are isolated on mica. The fact that

this doughnut morphology disappears in the case of the (800/83/50/40) copolymer can be attributed to the higher volume of the lateral side chains.

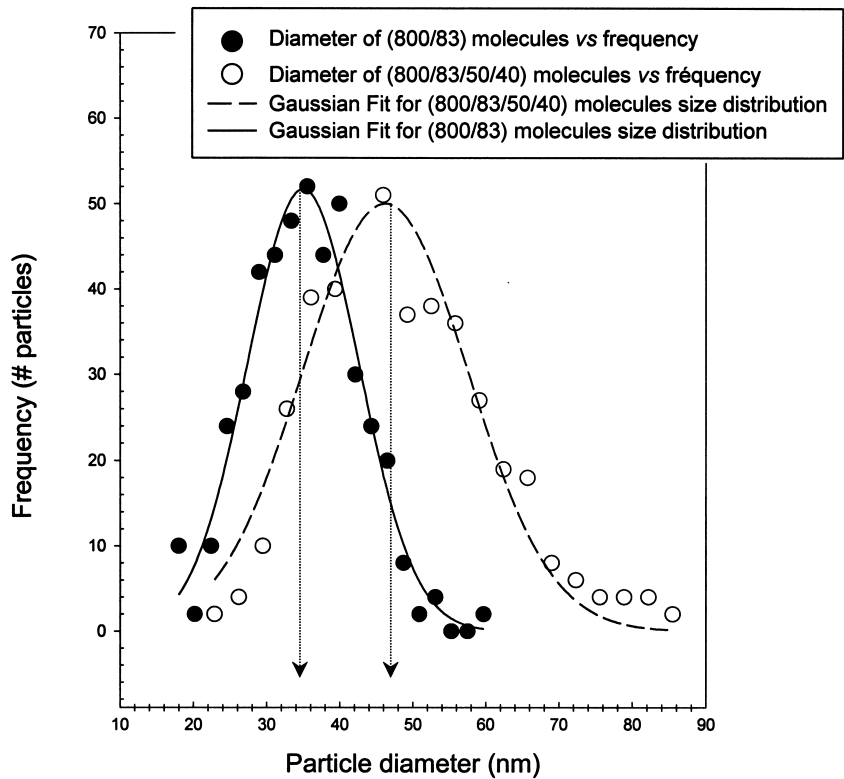


Fig. 9 : Diameter Gaussian distributions of individual copolymer molecules for the (800/83) copolymer and the (800/83/50/40) copolymer, respectively.

The individual copolymer molecules can also be analysed in terms of their heights. For instance, the measured height of (800/83) copolymer molecules found on the surface is 7 nm, which is in perfect agreement with the height of the corresponding monolayers shown in Fig. 5. This confirms once again that the layers appearing in the images of Fig. 5 are monolayers of the (800/83) copolymer.

Conclusions

Studying the surface organization of hyperbranched poly(chloroethyl vinyl ether-*g*-styrene) (PCEVE-*g*-PS) copolymer thin films, we have observed that the degree of lateral ordering of copolymer chains depends on their intrinsic molecular architecture, which leads the molecules to adopt a regular “cylindrical brush” conformation. The structural complexity and compactness of the lateral side chains strongly affects the surface molecular organization; AFM images show that an increase of this structural complexity causes the average cylindrical brush thickness to increase significantly.

In submonolayer deposits, AFM images also show very small objects whose size is coherent with that of single copolymer molecule. Again, the size evolution of these single molecules can be interpreted in terms of the complexity of their molecular architecture.

The “doughnut-like” morphology observed for isolated molecules of the less crowded copolymer probably originates from partial coiling of the PCEVE backbone, because of the weak affinity between the PS lateral chains and mica. In order to verify this behavior, the molecular organization of the copolymer molecules on other substrates, is currently under investigation.

Acknowledgments

This work was supported by the Government of the Region of Wallonia and the European Commission (Objectif 1-FEDER-NOMAPOL) and by the Belgian Federal Government Office of Science Policy (SSTC) “Pôle d’Attraction Interuniversitaire en Chimie Supramoléculaire et Catalyse Supramoléculaire” (PA/11). R.L. is Maître de Recherches du FNRS (Belgium).

References

1. Y. H. Kim, *J. Polym. Sci.: Part A: Polym. Chem.* **36**, 1685 (1998).
2. M. Freemantle, *Chem. Eng. News* **6**, 37 (1999).
3. A. Sunder, R. Mülhaupt, R. Haag, H. Frey, *Adv. Mater.* **12**, 235 (2000).
4. A. Deffieux, M. Schappacher, *Macromol. Symp.* **45**, 132 (1998).
5. A. Deffieux, M. Schappacher, *Macromolecules* **32**, 1797 (1999).
6. A. Deffieux, Z. Muchtar, M. Scappacher, *Polym Preprints* **41**, 1529 (2000)

7. S. S. Sheiko, M. Gerle, K. Fisher, M. Schmidt, M. Möller, *Langmuir* **13**, 5368 (1997).
8. M. Gerle, K. Fischer, S. Roos, A. H. E. Müller, M. Schmidt, S. S. Sheiko, S. Prokhorova, M. Möller, *Macromolecules* **32**, 2629 (1999).
9. G. H. Fredrickson, *Macromolecules* **26**, 2825 (1993).
10. P. G. de Gennes, *Macromolecules* **13**, 1068 (1980).